



Investigating the MHD current in presence of nanofluid inside a triangle duct in presence of electromagnetic field in form of Eulerian two phases

Amir Haghikhatkhan¹, Hossein Ahmadi Danesh Ashtiani^{2,*}, Kourosh Amiraslani¹

¹Department of Mechanical Engineering, Tehran South Branch, Islamic Azad University, Tehran, IRAN

²Assistant Professor of Energy and Mechanical Engineering, Faculty of Engineering, Tehran South Branch, Islamic Azad University, Tehran, IRAN

Received 06 Feb 2018,
Revised 22 May 2018,
Accepted 25 May 2018

Keywords

- ✓ heat transfer Nanofluid
- ✓ MHD current
- ✓ Nanofluid
- ✓ Nusslet
- ✓ Triangle channel
- ✓ Magnetic field

Email: haghikhatkhan.eng@gmail.com

Abstract

In order to increase the level of heat transfer in heat exchangers, using the Magneto hydrodynamic currents, channel cross section, and using nanofluids can be addressed. Over all, by presence of a magnetic field which covers the current inside the duct, fluids or particles which have magnetic characteristics will be affected and some forces in special directions will affect them. Using the MHD current, the current and heat transfer inside the pipes can be controlled in an arbitrary direction. In this research, the MHD current is investigated in presence of nanofluids inside a triangular duct and magnetic field in slow flow in form of completely two phases in Ansys CFX software. For this purpose, the external surface of channel gets cold or warm with a determined transmission coefficient and the effect of changes of Nusselt number also decrease of pressure for variable parameters like nanoparticles concentration, power of magnetic field, and shape of channel (relative to circular state) will be investigated.

1. Introduction

Many researchers make the channels with none circular cross section in some industries like automotive, power generation system, heating and air conditioning, chemistry engineering, Electronic chip cooling, space sciences, and In heat exchangers with different cross sections for input and output channels, the triangle type cross sections with equal sides create the maximum transmission cross section relative to volume [1]. In addition to cross section factor other factors are investigated which increase the heat transfer; one of the factors is using solid particles in operant fluid which create the nanofluid combination. The reason of increase of heat transfer by nanofluids is rising thermal conductivity coefficient of operant fluid relative to initial state [2]. Following the expressing the factors of heat transfer increase, use of Magneto hydrodynamic currents can be addressed. In recent years, because of extensive industrial applications, study of Magneto hydrodynamic current in electricity conductive fluids like liquid metals, extensively was center of attention of researchers. These currents in engineering and geophysics, control unwanted displacement currents through MHD generators design, metal casting processes, optimization of the crystal growth Process, plasma and nuclear reactors cooling industries, heat exchangers, cooling systems in electronic tools, solar collectors, cooling turbine rotors and high speed bearings. Using the MHD currents, the current and heat transfer inside the pipes can be controlled in arbitrary direction. In this research, a triangular channel in which the current is nanofluid in presence of magnetic field in slow flow in completely two phases form gets analyzed. For this purpose, the external surface of channel gets cold or warm with determined heat transfer coefficient and the effect of changes of Nusslet number and pressure drop for variable parameters like nanoparticles concentration, magnetic field power, and channel shape (relative to circular state) will be investigated.

2. Theoretical Foundation and Research Background

2.1. MHD current review

Generally, with presence of magnetic field which covers the current inside the duct, the fluid or particles which have magnetic characteristic will be influenced and some forces will be applied to them in an especial direction. The equations which model the intended behavior of magnetic field are called electromagnetic equations.

Generally electromagnetic equations are expressed by Maxwell's equations. These equations are a complex of four separate equations. These four equations together are known as material equations [3]:

1. Gauss's Law
2. Gauss's Law for magnetism
3. Faraday's Law of Induction
4. The Ampere's Law with Maxwell's correction

2.2. A review of Nanofluids

Xuan and Rotzel in [4] have suggested that with thermal equilibrium assumption between nanoparticles and base fluid and by neglecting the slip velocity between particles and fluid the nanofluid can be assumed as a single phase fluid with variable characteristics relative to volume fraction (α). By comparing the obtained results from these hypotheses with laboratory findings good compatibility is observed between obtained results. In this way since the amount of volume fraction is constant, they can be entered in equations solution in from of constant numbers, and it is not need to change it in different elements inside the duct and only after finding the volume fraction of nanoparticles their value will be determined and they will be entered to the problem.

- Nanofluid with non-uniform volume fraction

This state is more complex than the first state, because, first it is not possible to use single phase model any more, second it is not possible to assume that the characteristics are constant any more, and they must be entered in problem parametrically (in other word, for each element inside the pipe different characteristics must be intended). In this state, for analyzing the current and heat transfer in all of the regions of the pipe the two phase current method will be used. The two phase currents get modeled with these two following methods:

Eulerian-lagrangian method: the base of assumptions which are intended in this method are according to this, that the diffused second phase in fluid current take low volume unless the mass of it be high (particle $m \geq$ fluid $>w$ volume unless the mass of it be high (prticle rent take lwsed on this e that the characteristics are constant any more and $27042704m^\circ$), in this method the trajectory of solid particles or the liquid drops get calculated uniquely in determined time interval during calculating the phase of fluid [5]. Eulerian-eulerian method: this model has three solution methods: A) VOF model, B) mixture model, and C) Eulerian model.

In this study the Eulerian method will be used. In this model the both two phases are considered as continuous fluid and n series of momentum and continuity equations get resolved, coupling of these equations are achieved by exchanging the coefficients of intermediate phase and pressure.

3. Equations and Mathematical Relations

3.1. thermophysical characteristics of nanofluid used in this research

Corcione [6] has provided the empirical relationship of dynamic viscosity based on a lot of empirical data as following:

$$\frac{\mu_{eff}}{\mu_{bf}} = \frac{1}{1 - 34.87 \left(\frac{d_p}{d_{bf}}\right)^{-0.3} \phi^{1.03}}, \quad (1)$$

In which the μ_{eff} is the dynamic viscosity of nanofluid, the μ_{bf} is the dynamic viscosity of base fluid, and the d_{bf} is the equivalent diameter of base molecule of liquid which is obtained by following relation:

$$d_{bf} = 0.1 \left[\frac{6M}{N\pi\rho_{bf}} \right] \quad (2)$$

In which the M is the molecular weight of base fluid, the N is the Avogadro number, and the ρ_{bf} is mass density of base fluid in $T=293$ k temperature. The effective thermal conductivity of nanofluid relationship is provided by Koo and Kleinstreuer [7] and is more developed by Vajjha and Das [6]. The effective thermal conductivity is provided as following:

$$k_{eff} = k_{Static} + k_{Brownian} \quad (3)$$

$$k_{Static} = k_{bf} \left[\frac{k_p + 2k_{bf} + 2\phi(k_p - k_{bf})}{k_p + 2k_{bf} - \phi(k_p - k_{bf})} \right] \quad (4)$$

$$k_{Brownian} = 5 \times 10^4 \beta \phi \rho_{bf} C_{pbf} \sqrt{\frac{kT}{\rho_p d_p}} f(T, \phi) \quad (5)$$

$$f(T, \phi) = (2.8217 \times 10^{-2} \phi + 3.917 \times 10^{-3}) \left(\frac{T}{T^\circ}\right) + -3.0669 \times 10^{-2} \phi - 3.91123 \times 10^{-3} \quad (6)$$

The $f(T, \phi)$ is temperature and volume fraction function of particle. The β is the volume function of liquid which moves by the particle which is provided in Table 1.

Table 1: the relationships of appropriate curve suggested by Vijjha and Das [6,7]

Type of particles	β	Concentration rate (%)	Temperature rate (k)
Al₂O₃	$8.4407(100\phi)^{-1.07304}$	$1 \leq \phi \leq 10$	$298 \leq T \leq 363$
CuO	$9.881(100\phi)^{-0.9446}$	$1 \leq \phi \leq 6$	$298 \leq T \leq 363$
SiO₂	$1.9526(100\phi)^{-1.4594}$	$1 \leq \phi \leq 10$	$298 \leq T \leq 363$

The effective density of nanofluid is expressed as following by Pak and Cho [8]:

$$\rho_{eff} = \phi\rho_p + (1 - \phi)\rho_{bf} \quad (7)$$

The Xuan and Rotzel equation is used for calculating the specific heat of nanofluid like thermal balance between nanoparticles and liquid:

$$C_{p_{eff}} = \frac{(1 - \phi)(\rho C_p)_{bf} + \phi(\rho C_p)_p}{(1 - \phi)\rho_{bf} + \phi\rho_p} \quad (8)$$

3.2. MHD current modeling and final equations

Generally, the electromagnetic equations are expressed by Maxwell equations. These equations are a complex of four separated equation. These equations along with each other are known as material equations. In following these four equations are introduced and their relationships is expressed [9,10].

1. Gauss's Law

$$\nabla \cdot \vec{B} = 0 \quad (9)$$

2. Gauss's Law for magnetism

$$\nabla \times \vec{E} = -\frac{\partial \vec{B}}{\partial t} \quad (10)$$

3. Faraday's Law of Induction

$$\nabla \times \vec{H} = \vec{j} \quad (11)$$

4. The Ampere's Law with Maxwell's correction

$$\nabla \cdot \vec{D} = 0 \quad (12)$$

There are some relations for above equations that can be expressed in following form:

$$\vec{H} = \frac{1}{\mu_m} \vec{B}, \quad (13)$$

$$\vec{j} = \sigma(\vec{E} + \vec{V} \times \vec{B}) \quad (14)$$

$$\vec{D} = \epsilon \vec{E} \quad (15)$$

By combining the above equations the magnetic field equation for each fluid is obtained in following form:

$$\frac{\partial \vec{B}}{\partial t} + (\vec{V} \cdot \nabla) \vec{B} + (\nabla \cdot \vec{V}) \vec{B} = (\vec{B} \cdot \nabla) \vec{V} + \frac{1}{\mu_m \sigma} \nabla^2 \vec{B} \quad (16)$$

In above relations B is magnetic field, μ_m is magnetic permeability, σ is electric conductivity coefficient, E is electric field, ϵ is environment permeability coefficient and V is the velocity of current [11].

Based on electromagnetic theory while a fluid is in electromagnetic field a force named Lorentz force is applied to it. Therefore, by attention to equation (8) it can be said that magnetic and electric fields and current are coupled with each other.

3.3. The geometry of problem and boundary conditions

The geometry of the examined issue contains a triangular channel which its cross section is equilateral with side w and its length is L, figure 1. The boundary conditions on the walls of this channel are in Table 2.

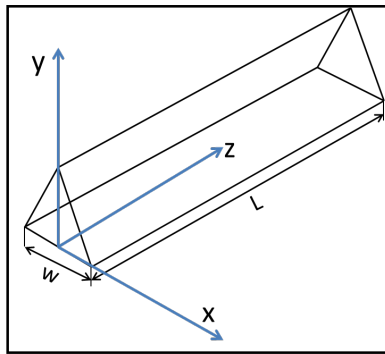


Figure 1:The geometry of the examined issue in present research

Table 2:boundary conditions of present issue based on figure 1

Boundary conditions	assumptions
input	$\frac{\partial u}{\partial z} = \frac{\partial v}{\partial z} = \frac{\partial w}{\partial z} = \frac{\partial T}{\partial z} = 0, z/L = 0$
output	$\frac{\partial u}{\partial z} = \frac{\partial v}{\partial z} = \frac{\partial w}{\partial z} = 0, \frac{\partial T}{\partial z} = 0, z/L = 1$
Steep walls (non-slip)	$u = v = w = 0, T = T_w = 330 K$
Bottom wall (adiabatic)	$u = v = w = 0, \frac{\partial T}{\partial y} = 0$

4. Numerical Modeling

4.1. Simulated data

The geometry of the issue with boundary conditions is expressed in previous section, but in this section in addition to completing the information of issue geometry, other input parameters are provided in table 3 for simulation. It is worth to mention that the geometry of issue contains three channels that are in series with each other that only the middle channel has the value of analyzing the information and two input and output channels only are used for satisfying zero gradient boundary condition in two input and output bound; the geometry is provided in figure 2.

Table 3:Important parameters in the problem.

The name of parameter	Symbol	Unit	value
The side of the equilateral triangle	W	m	0.01
Hydraulic diameter	D_h	m	0.0057735
Main channel length	L	m	0.1454
Channel input length	L_{entrance}	m	0.1155
Output length	L_{outlet}	m	0.05
Particles diameter	d_p	Nm	25
Particles material			Al2O3
Volume fraction of particles	Φ	%	1 TO 4
Reynolds number	Re		100 TO 800
Input fluid temperature	T_{inlet}	K	300

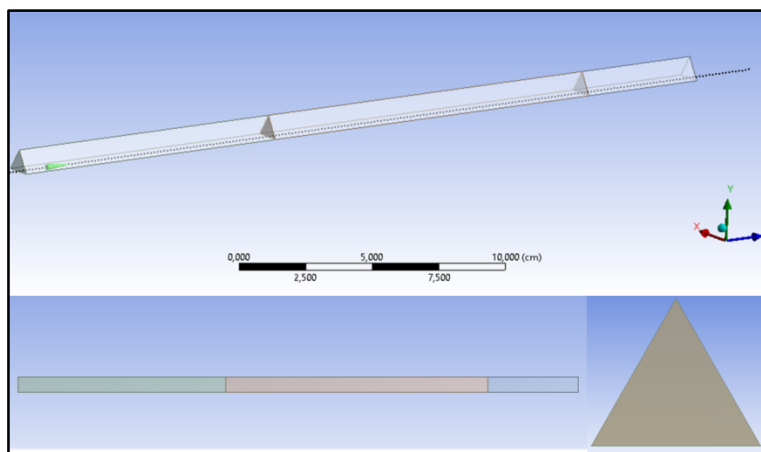


Figure 2:an image from three view of investigated geometry, three main, input, and output channels.

4.2. Networking and independence of the network

The AnsysMeshing tool is used for meshing. It has been tried to equilateral triangle be mesh and swept along the axis of channel. In figure three image of organized network used in this project can be seen.

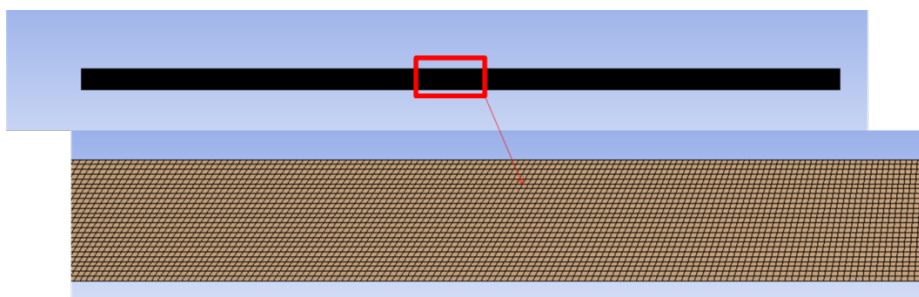


Figure 3:an image of done network

In order to investigate the independence from network the mean Nusslet number is presented in table 4 for networking with different size. As it can be seen in Table the mesh with 350000 elements for simulation of the problem is convenient.

Table 4:investigating the changes of results by changing the size of elements

Mean Nusslet number	Number of elements
3.144	34000
3.162	87000
3.157	150000
3.156	350000
3.157	750000

4.3. Verifying the correctness of results

In order to verify the correctness of results the existing simulations and laboratory results for current inside the triangle channel is used, one of these references is Saeed et al, [11]. As it can be seen in figure 4 the difference between the obtained results with provided results in mentioned reference is negligible.

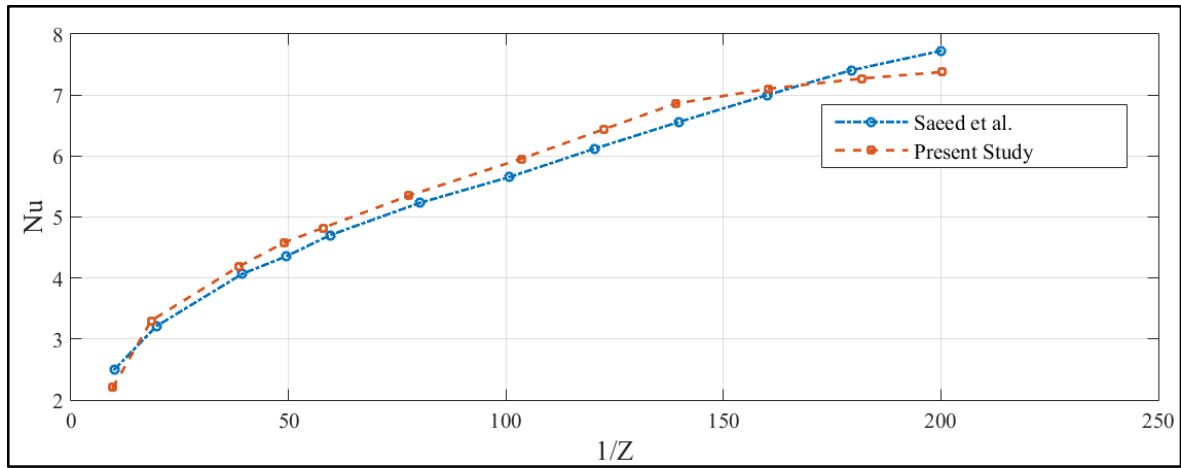


Figure 4: Comparing the obtained data of simulation in present study with reference

5. Results and discussion

In following some of the results of simulation is provided, because of low importance of some of the results, they are provided only for one characteristic (for example the percentage of particle concentration).

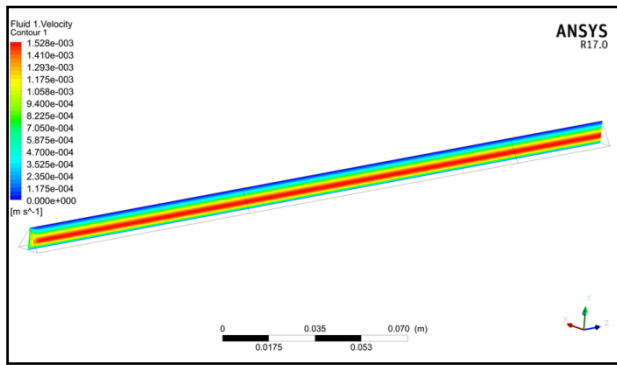


Figure 6: Water velocity contour, Al₂O₃ particles with a concentration of 4%

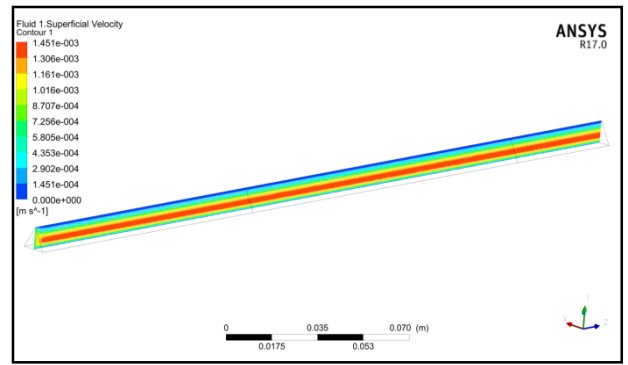


Figure 5: Water relative velocity contour, Al₂O₃ particles with a concentration of 4%

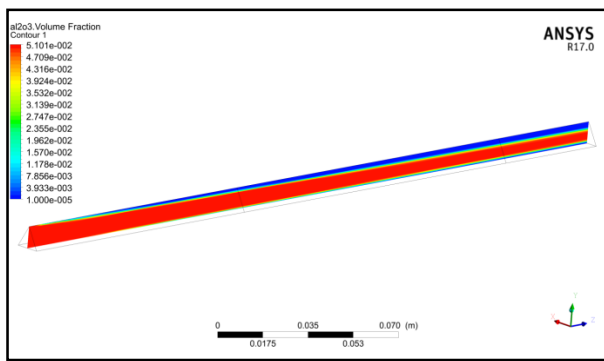


Figure 8: volume fraction contour of Al₂O₃ particles with a concentration of 4%

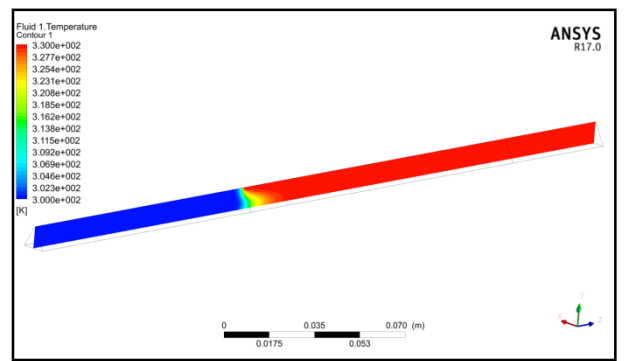


Figure 7: Water temperature contour with Al₂O₃ particles with a concentration of 4%

In figure 5, contour of relative velocity for water fluid with Al₂O₃ particles with the size of 4% of mass fraction is illustrated. As it can be seen the relative velocity of two phases relative to each other are close to zero in the regions next to the corner of the triangle. As the movement gets close toward the walls, this relative velocity increases. At the end this value has decreased again. As it can be seen in figure 6 the velocity of water in the regions next to the corner of triangle is close to zero. As the movement gets close toward the walls, this velocity increases and at the end this value decreases by being contiguous with the wall opposite the corner. In figure 7 the contour of temperature for water fluid with AL₂O₃ particles with the size of 4% of mass fraction is shown. As it can be seen the temperature of water has reached to the temperature of wall quickly after entering of fluid

to main region. As it can be seen in figure 8 the volume fraction in the regions next to the corners of triangle is close to zero, and as the movement gets toward the walls, this value increases and at the end by getting closed to the wall opposite the corner this value decreases again.

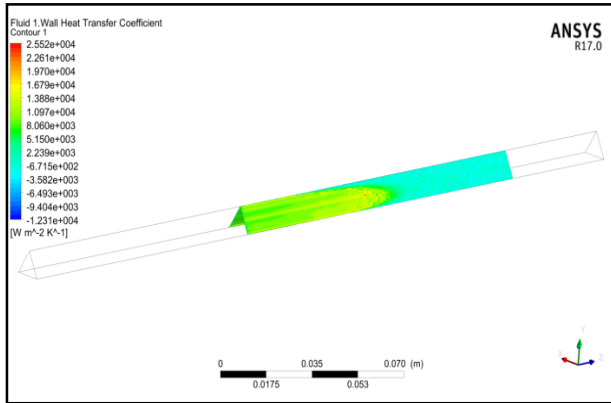


Figure 10: Heat transfer coefficient on the main channel wall contour for water, volume fraction of Al₂O₃ particles with a concentration of 4%

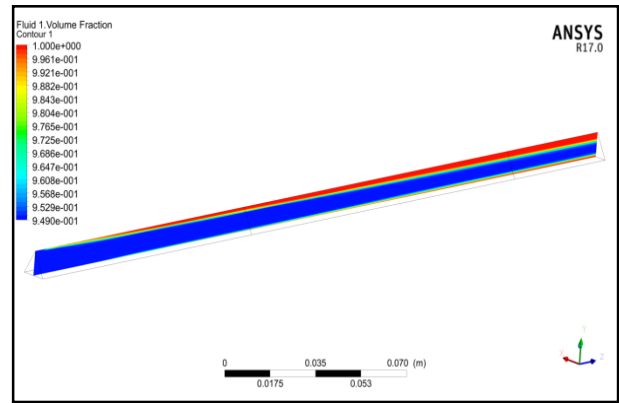


Figure 9: mass fraction contour of water with Al₂O₃ particles with a concentration of 4%

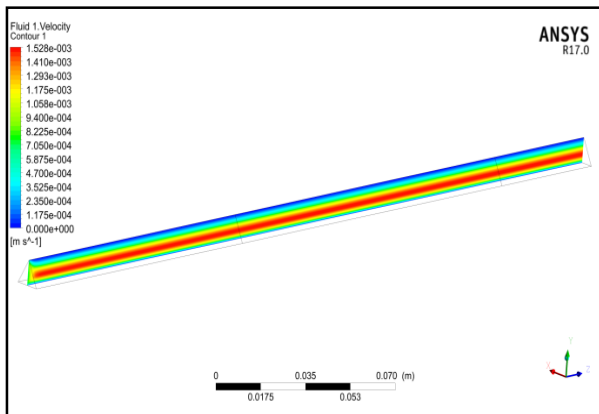


Figure 12: water velocity contour all over the channel, mass fraction contour of Al₂O₃ particles with a concentration of 4%

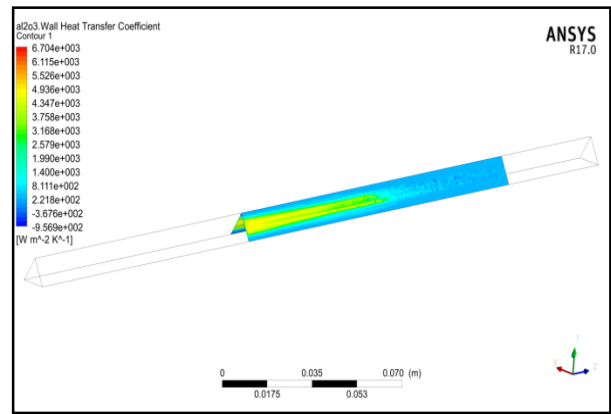


Figure 11: Heat transfer coefficient contour on the main channel wall for Al₂O₃, volume fraction of Al₂O₃ particles with a concentration of 4%

In figure 9 volume fraction of water is shown. As it can be seen the volume fraction in the regions next to the corners of triangle is close to 1, and as the movement gets close to the walls this value decreases and at the end by getting close to the wall opposite the corner this value increases again. As it can be seen in figure 10, the heat transfer coefficient in beginning of entering to the main channel has lower value and then increases and again decreases quickly. The contour of heat transfer coefficient for Al₂O₃ particles for main channel with Al₂O₃-water nanoparticle with volume fraction of 4% is illustrated in figure 11. As it can be seen this value in beginning of entering to the channel was more and then decreases. As it can be seen in figure 12 the velocity of water in the regions next to the corners of triangle gets closed to zero. As the movement gets close to the walls this velocity increases and at the end this value decreases again by being contiguous with the wall which is opposite to the corner.

As it can be seen in figure 13 by increase of Reynolds number the value of heat transfer coefficient of surface increases in average, moreover, the changes from single phase model to two phase leads to increase of heat transfer coefficient [12]. At the end it is clear that by increase of volume fraction of particles inside the nanofluid the amount of heat transfer can be increased. The figure 14 shows that by moving along the channel the amount of heat transfer coefficient first increase and then decrease. Moreover, it is clear that by increase of volume fraction of particles inside the nanofluid the amount of heat transfer can be increased. In figure 15 the curve of velocity inside the channel is illustrated in dimensionless form with entering velocity relative to dimensionless path from the center of the triangle to the corner. As it is obvious by increase of volume fraction, velocity profile has less change in center and there are increase of velocity gradient and consequently increase of friction over the wall [13].

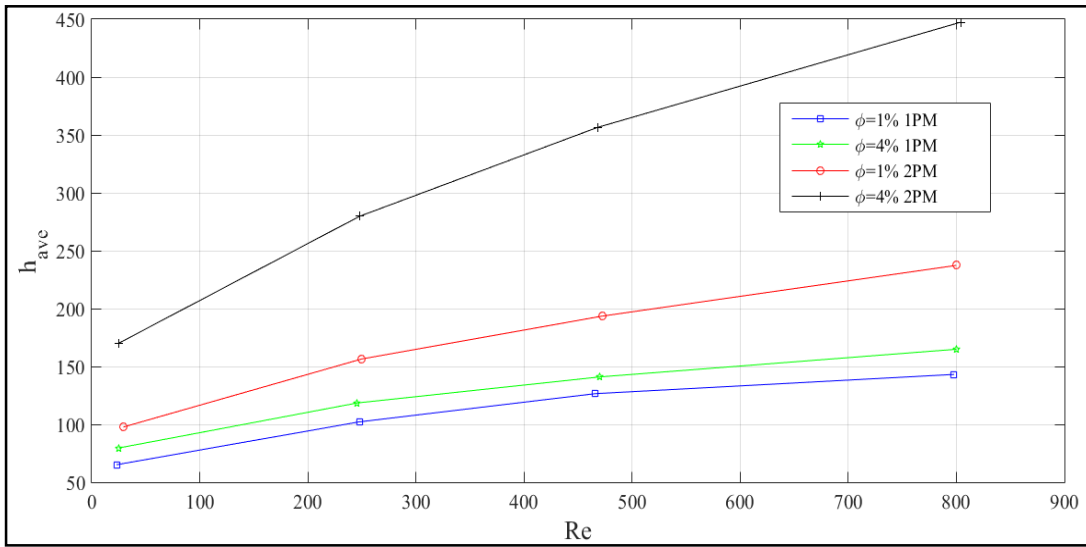


Figure 13: changes of surface heat transfer coefficient with Reynolds number in different volume fractions for 1 phase model (1pm) and two phases model (2pm)

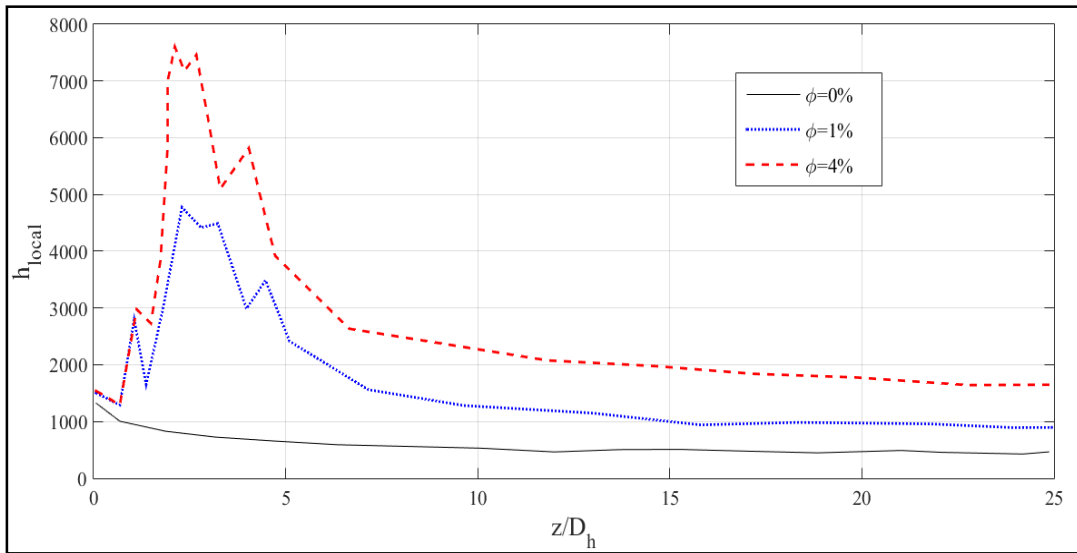


Figure 14: Changes of heat transfer coefficient along the channel for different volume fractions by two phases model

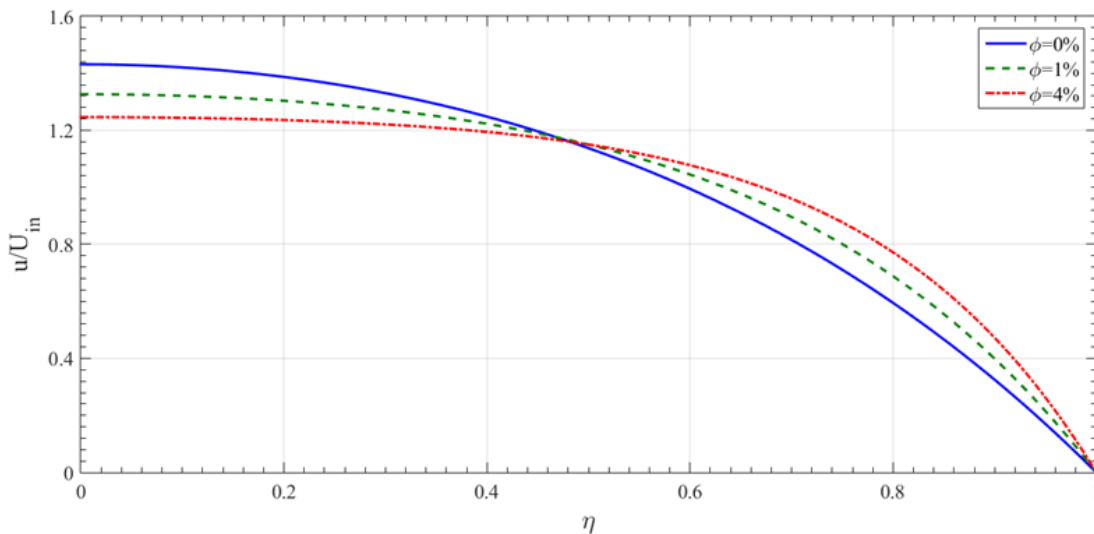


Figure 15: the effect of change of volume fraction in dimensionless velocity relative to distance from center of channel up to the wall.

- Magnetic field effect

By applying a magnetic field with power of B in center of main channel and by defining Hartmann number in form of ration of magnetic force to viscose force, the effect of increase of decrease of magnetic field on dynamic and thermal parameters can be observed.

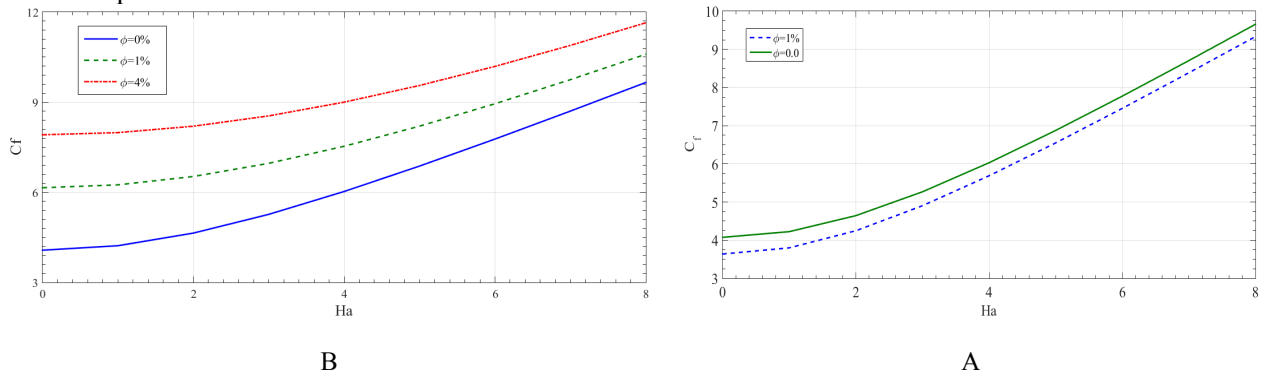


Figure 16: The effect of magnetic field (Hartmann number) on friction coefficient for different volume fraction for A) single phase model and B) two phases model

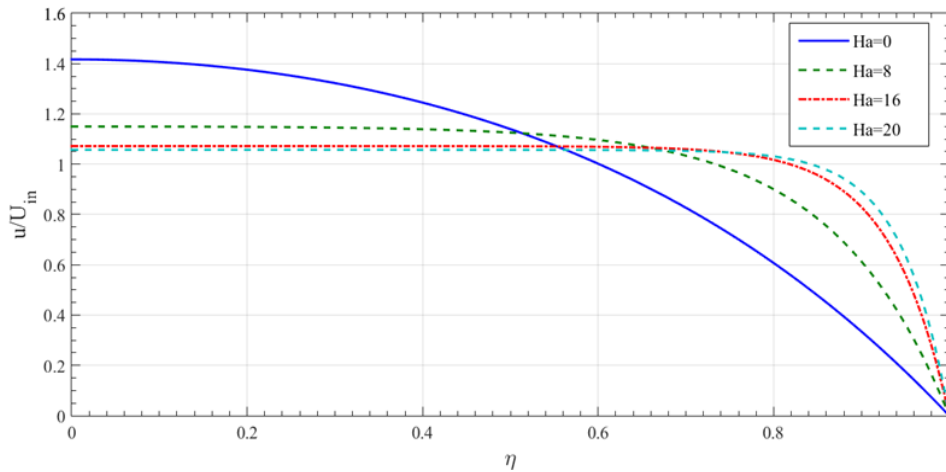


Figure 17: The effect of Hartmann number on dimensionless velocity in the distance from center of channel up to the wall for different volume fractions of two phase model.

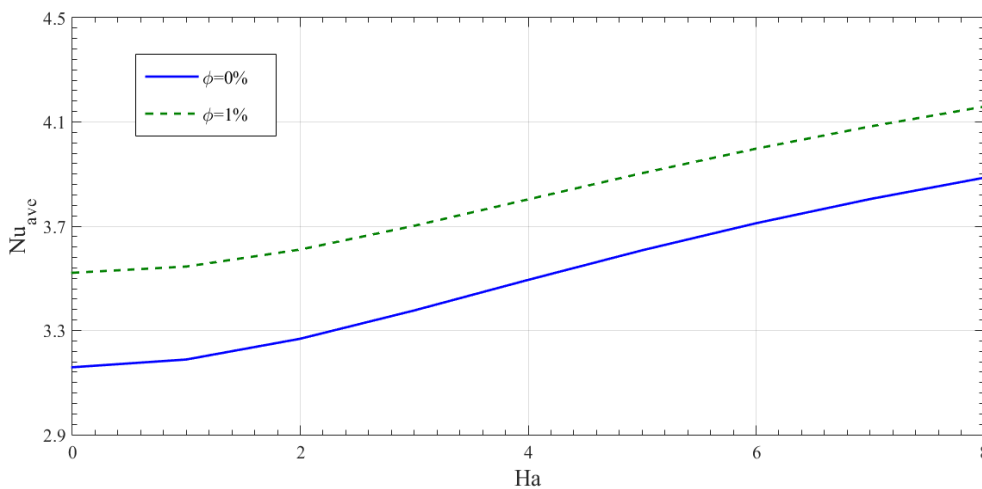


Figure 18: the effect of magnetic field (Hartmann number) on mean Nusslet number in the distance from center of channel to the wall for different volume fractions of two phase model.

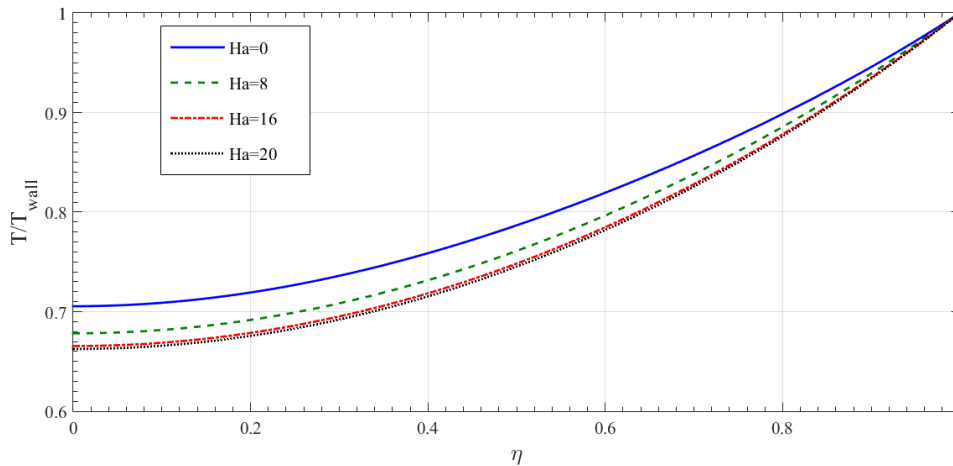


Figure 19: the effect of magnetic field (Hartmann number) on dimensionless temperature in the distance from center of channel to the wall for different volume fractions of two phase model.

Conclusions

In this research, a triangle channel in which there is current of a nanofluid in presence of magnetic field with slow flow in form of completely two phases is investigated. For this purpose, the external surface of channel gets warm with determined heat transfer coefficient and the effect of changes of thermal and fluid parameters are observed by changes in engaged parameters in issue.

- The result of magnetic field use

Because of use of magnetic field, considerable changes have occurred in behavior of current which include following cases:

- By increase of magnetic field and consequently Hartmann number, friction coefficient increases, it is due to increase of shear stress on the wall by increase of magnetic field.
- The velocity inside the triangle channel increase with more slop by increase of magnetic field and this factor leads to increase of velocity gradient and consequently increase of shear stress over the wall.
- By attention to increase of velocity gradient created by increase of magnetic field power, the amount of heat transfer in surface increases and as a result the mean Nusslet number over the surface increases. This factor leads to decrease of temperature on wall which over all is the sign of increase of performance of system in heat transferring.
- By increase of magnetic field power the profile of velocity have less change in center and there are increase of velocity gradient and consequently friction increase over the wall.

- Moving along the channel

- By moving along the channel amount of the heat transfer coefficient first increase then decrease. Moreover, it is clear that by increase of volume fraction of particles inside the nanofluid the amount of heat transfer can be increased.
- Shear rate over the channel through wall of channel first increase then have a decreasing trend.
- The velocity of nanofluid mixture in the regions next to corners of triangle is close to zero also as movement gets close to wall this velocity increase and at the end this value by being contiguous to the wall opposite to the corner decrease.
- Heat transfer coefficient for Al₂O₃ over the wall of channel is such that first it increase and then gradually by getting close to middles of the path it get decreased and travel with a constant amount.
- Heat transfer coefficient for water over the wall of the channel is such that in the beginning of entering to main channel have less value and then increase and again quickly decrease.
- Volume fraction of Al₂O₃ in the regions next to corners of triangle is close to zero and as the movement gets close to wall this value increase and at the end by getting close to the wall opposite to corner this value decrease again.
- Volume fraction of water in the regions next to the corners of triangle is close to 1 and as movement gets close to walls this value decrease and at the end by getting close to the wall opposite to the corner this value increase again.

- Mass fraction
- There is a difference between the results of single phase modeling and two phase modeling, for example in single phase modeling friction coefficient have considerable difference with two phase modeling.
- By increasing the Reynolds number surface heat transfer coefficient increase in average, also changes from single phase model to two phase model leads to increase of heat transfer coefficient, at the end it is clear that by increase of volume fraction of particles inside the nanofluid heat transfer can increase.

References

1. C.A.C. Altemani, EM. Sparrow, Turbulent heat transfer and fluid flow in an unsymmetrically heated triangular duct. *J Heat Transf* 102 (1980) 590–597.
2. HE. Ahmed, MZ. Yusoff, MNA. Hawlader, MI. Ahmed, Numerical Analysis of Heat Transfer and Nanofluid Flow in a Triangular Duct with Vortex Generator: Two-Phase Model. *J Heat Transf* 0 (2014), 1-21.
3. J. D. Jackson, Classical Electrodynamics, JohnWiley & Sons, New York. NY, USA, 2nd edition, (1975).
4. Y. Xuan, W. Roetzel, Conception for heat transfer correlation of nanofluids, *Int. J Heat Mass Transfer*, 43 (2000), 3701-3707.
5. Patankar, N. A., Joseph, Modeling and numerical simulation of particulate flows by the Eulerian-Lagrangian approach. *Int. J. Multi. Flow* 27 (2001) 1659.
6. V. Vasu, K.R. Krishna, A.C.S. Kumar, Application of nanofluids in thermal design of compact heatexchanger, *Int J Nanotechnol Appl*. 2(1) (2008) 75–87.
7. A. Behzadmehr, M. Saffar-Avval, N. Galanis, Prediction of turbulent forced convection of a nanofluid in a tube with uniform heat flux using a two phase approach. *Int J Heat Fluid Flow* 28 (2007) 211–219.
8. R. Lotfi, Y. Saboohi, A.M. Rashidi, Numerical study of forced convective heat transfer of Nanofluids:comparison of different approaches. *Int Commun Heat Mass Transf*. 37 (2010) 74–78.
9. M. Kalteh, A. Abbassi, M. Saffar-Avval, A. Frijns, A. Darhuber, J. Harting, Experimental and Numerical investigation of nanofluid forced convection inside a wide microchannel heat sink. *Appl. Therm Eng.* 36 (2012) 260–268.
10. J. D. Jackson, Classical Electrodynamics, JohnWiley & Sons, New York. NY, USA, 2nd edition, (1975).
11. Saeed ZH, Seyyed HN, Elham T, Javad S. Numerical investigation of Al₂O₃/water nanofluid laminar convective heat transfer through triangular ducts. *Nanoscale Res Lett* 6 (2011) 1–10.
12. A. Akbarzadeh, F. Talati, A. Paykani. Effect of radiation heat transfer on HCCI multizone combustion. *Heat Transf. Res.* 45(1) (2014) 23-41.
13. A Paykani, R Khoshbakhti Saray, AM Kousha, MT Shervani Tabar, Performance and emission characteristics of dual fuel engines at part loads using simultaneous effect of exhaust gas recirculation and pre-heating of in-let air. *Int. J. Automotive Eng.* 1(2) (2011) 53-67.

(2018) ; <http://www.jmaterenvirosci.com>